Received: 3 March 2023 | Revised: 13 April 2023 | Accepted: 4 May 2023

DOI: 10.1002/est2.484

RESEARCH ARTICLE

ENERGY STORAGE WILEY

Multi objective queue theory based optimal planning of rapid charging stations and distributed generators in coupled transportation and distribution network

Vutla Vijay | **Chintham Venkaiah** | **D. M. Vinod Kumar**

Department of Electrical Engineering, National Institute of Technology, Warangal, India

Correspondence
Vutla Vijay, Department of Electrical Engineering, National Institute of Technology, Warangal, Hanumakonda, India.
Email: vutlavijay.99@gmail.com

Abstract

The environment is adversely affected by greenhouse gas (GHG) emissions from conventional combustion engines. In this regard, electric vehicles (EVs) are a viable transportation option that benefit the environment in reducing GHG emissions. Although the installation of rapid charging stations (RCSs) helps to promote EVs, installing these at improper locations in the distribution network worsens the voltage profile, increases power loss, and energy loss while travelling from EV's current location to RCS. Furthermore, RCS installation cost and waiting time at RCS need to be considered. Therefore, a two-stage optimal planning is proposed in this article to address the issues stated above. In the first stage, simultaneous optimal planning of RCS and distributed generators is done to minimize active power loss, voltage deviation, EV user cost and to maximize voltage stability index. In the second stage, optimal number of connectors are decided to minimize the installation cost and waiting time in queue at RCS. Here, M1/M2/C queuing model is considered to determine the waiting time. A test network of coupled IEEE 33 bus distribution system and transport network is proposed to validate the proposed methodology. Multi objective Rao algorithm (MORA) is used to solve the formulated optimization problems, and results are compared with non dominated sorting genetic algorithm (NSGA-II) algorithm.

KEYWORDS

coupled network, distributed generator (DG), multi objective Rao algorithm (MORA), queuing theory (QT), rapid charging stations (RCS)

1 | INTRODUCTION

The use of electric vehicles (EVs) for transportation has been increasing in recent years. Adopting EVs for transportation can reduce CO_2 emissions from 50 to 100 g per mile.[1] Customers are interested in EVs for transportation due to government initiatives, the reduction of fossil fuels, and rising oil prices. As a result, the population of EVs has increased by 1.5% in China, 6.5% in Netherlands, and 28.8% in Norway. However, longer charging times and shorter driving ranges will impact EV adoption.

The challenges posed by short driving range can be mitigated by installing adequate charging infrastructure. There are mainly three charging methodologies, namely, Type 1, Type 2, and Type 3. Type 1 and 2 take more time for charging, whereas Type 3 is DC Rapid charging methodology, which takes less time. However, integrating RCS may create technical problems for the power system

due to increased system load.[2,3] Voltage deviations, component overloading, and higher system losses are a few of them. The design and feasibility analysis of charging station (CS) was done in Reference 4 with the considerations of different configurations and techno-economic performance. Integration of RCS has a significant influence on distribution sysytem (DS) and this may lead to adverse impact if RCS were located at improper places.[5,6]

The presence of a CS in the distribution system increases power loss and voltage deviation. As improper locations increase severity, the authors in Reference 7, placed CS at optimal locations to improve the DS performance. Sometimes a combination of slow and fast charging connectors are needed at the same charging station. In Reference 8, installation of level 1, level 2, and level 3 connectors was done at CS. Though the CS is located at proper places, high loading on DS cause the increase in power loss and voltage deviation. Integrating the DGs into the DS could improve the DS performance. In Reference 9, optimal placement of CS and solar power DGs has been done by considering the CS investor decision index, land cost index and EV population index. In Reference 10, the authors used a hybrid meta-heuristic algorithm to identify CS locations with randomly distributed PVs in DS. These authors considered the minimization of power loss, voltage deviation, and voltage stability index (VSI) as objectives. In Reference 11, the authors proposed a methodology to optimally plan CS, DGs, and shunt capacitors (SCs). Integration of SC reduced power loss and improved voltage profile. In Reference 12, the authors proposed hybrid grey wolf optimizer and PSO algorithm to optimally locate (electric vehicle charging station) EVCS and DGs in a distribution system. Authors in Reference 13 used demand side management approach for coordination of DGs, battery energy storages, and photo voltaic sources in the presence of EVs. In Reference 14, the authors used the Arithmetic Optimization Algorithm for optimal planning of CSs and DGs. In the aforementioned literature, a distributed system is used as a test system. However, the transportation network also plays a key role in determining optimal CS locations.

From a user and utility perspective, consideration of the road network ensures a superior site. In planning for CS, very few authors have considered the transportation network.[15-19] To plan a CS near an existing CS, the author in Reference 15 suggested a two-level method. The minimization of power loss, voltage deviation, and CS installation cost were considered as objectives. The authors of Reference 16, proposed a method for CS and wind based DG planning while minimizing power loss, voltage deviation, and EV user cost. The optimal planning of fast CSs and DGs has been done simultaneously in the coupled network to minimize installation cost and to improve the performance of distribution system in Reference 17. In Reference 18, the authors applied enhanced heuristic descent gradient (EHDG) and Voronoi diagram to optimally plan CSs by considering route distributions, consumption profile, and operating cost. In Reference 19, the authors proposed a strategy to place CSs at optimal locations in a coupled network by minimizing land cost, power losses, voltage deviations, and to maximize the serving of CS. In Reference 20, the authors proposed a multi objective approach to determine the optimal locations for CSs. Probabilistic load modelling is used to capture the uncertainty of EVs and electric demand.

Queuing theory was rarely used by authors in the domain of EVs. By using a queuing analysis, the authors of Reference 21 modelled the load of plug-in EVs. The authors only considered the transportation system while determining the position and size of the CS in Reference 22. The authors in Reference 23, suggested a queue theory-based CS planning by minimizing power loss, EV user cost, installation costs, and maximizing VSI for the coupled network. In Reference 24, the waiting time at CS was minimized together with power loss, voltage deviation, and accessibility index. However, DG installation can further enhance the performance of distribution system.

In the literature,[7-12] the authors considered only distribution system,[15-19] authors considered coupled network for CS placement. Most of the articles considered the minimization of power loss and voltage deviation (VD) in optimal planning of RCS. But voltage stability not only depends on voltage deviation, but also VSI. Moreover, very few authors have considered the maximization of VSI as an objective. Furthermore, consideration of maximum connectors at RCS is not an economic approach. But the reduction in connectors increases the waiting time at RCS. To solve the above issues optimal planning of RCS and DGs has been done in two stages. Optimal location of RCS and optimal planning of DGs has been done in the first stage by minimizing power loss, voltage deviation, EV user cost and maximizing VSI. Optimal number of connectors was identified in second stage to minimize the waiting time in queue and installation cost of RCS. The PSO, chicken swarm optimization, grey wolf optimization, and different hybrid algorithms were the most often employed algorithms in the literature. The parameter tuning determines both the accuracy and the convergence speed. Thus, a novel multi objective Rao algorithm (MORA) is employed in this article to determine the optimal solutions.

The contributions of this article are listed below:

- For the best planning of RCS and DGs, the coupled network of electrical distribution and road transportation network is taken into account.

- The suggested two stage strategy yields the best size and locations of RCS and DGs.
- Minimization of EV user cost and maximization of VSI are considered along with the minimization of power loss and VD in Stage 1.
- In Stage 2, the application of queuing theory was employed to determine the optimal number of connectors at RCS by minimizing waiting time in queue at RCS and RCS installation costs.
- MORA is used for solving the formulated objective function and results are verified with the outcomes of non dominated sorting genetic algorithm (NSGA-II).

The structure of the article is as follows. Section 2 formulates the objectives of the problem under consideration. The MORA and the flowchart of the proposed approach are described in Section 3. The discussion on the simulated results is reported in Section 4 and a summary of the article figures in Section 5.

2 | PROBLEM FORMULATION

This section presents two stage approach for optimal planning of RCS and DGs in a coupled network, objective functions, operational constraints considered in each stage, DG modelling, and RCS modelling.

2.1 | Two stage approach

In this article, optimal planning of RCS and DGs has been done in two stages (Figure 1). Integration of only RCS into the distribution system cause the performance degradation. In this context, DG integration is adopted and analysed the test system in Stage I. Based on the results achieved from Stage I, optimal number of connectors are determined in Stage II to benefit EV user and RCS owner.

2.1.1 | Stage I: Optimal location of RCS and optimal location and sizing of DGs in a coupled network

In Stage I, optimal locations of RCS and optimal planning of DGs has been done through two scenarios. In Scenario 1, the impact of RCS on the performance of distribution system is analysed through various cases (explained in Section 4.2.1). In Scenario 2, concurrent optimal planning of RCS and DGs is done and analysed the performance of distribution system through various cases (explained in Section 4.2.2). Optimal sitting of RCS, optimal sitting and sizing of DGs were done by minimising of power loss (P_{loss}), maximum voltage deviation (MVD), EV user cost (EVUC), and maximizing the VSI. Equation (1) shows the objective function in Stage I, where feasible locations of RCS (l_{RCS}), locations of DGs (l_{DG}), and size of DGs (S_{DG}) were the decision variables.

$$f(l_{\text{RCS}}, l_{\text{DG}}, S_{\text{DG}}) = \min(P_{\text{loss}}, \text{MVD}, \text{EVUC}, (1/\text{VSI})) \quad (1)$$

Here, certain constraints exist while planning the RCS and DGs optimally in the coupled network. Feed forward and backward sweep algorithm is used for load flow study to achieve the power loss, node voltages, and VSI.

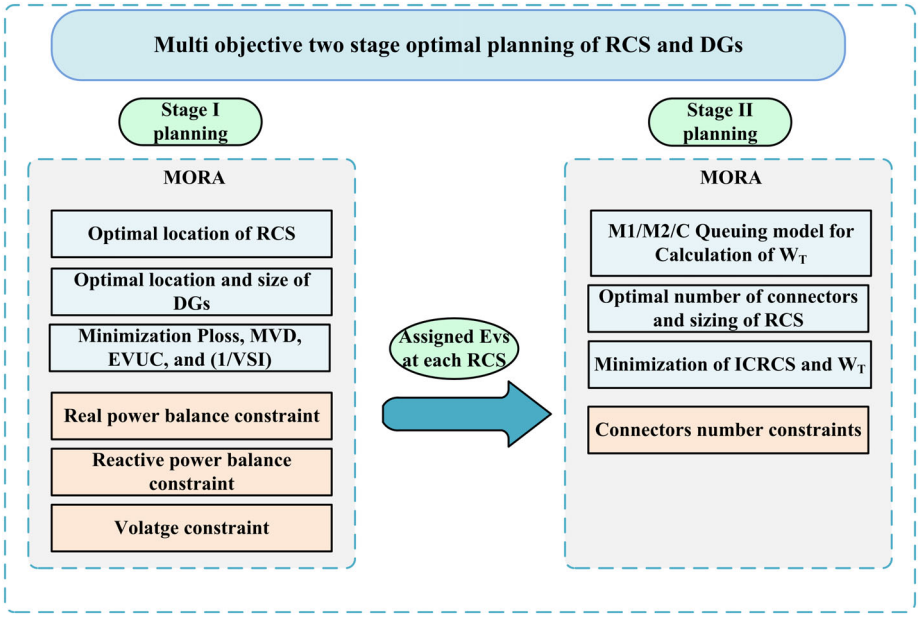

FIGURE 1 Proposed two stage model for optimal planning of RCS and DGs.

While planning RCS and DGs in a coupled network optimally in Stage I, few equality and inequality constraints are considered. The real and reactive power balance in the distribution system is considered using Equations (2) and (3). Addition of the RCS results in deterioration of voltage profile. Hence, to maintain voltage limits, Equation (4) was used as constraint. DGs minimum active power limits and total active power supplied by all DGs were used as constraints using Equations (5) and (6), respectively. In Equation (6), the contribution from all DGs was limited by minimum active power consumption over a 24 h period.

$$P_{\text{sub}} + \sum P_{\text{dg}} = P_{\text{D}} + \sum P_{\text{RCS}} + P_{\text{loss}} \tag{2}$$

$$Q_{\text{sub}} + \sum Q_{\text{dg}} = Q_{\text{D}} + \sum Q_{\text{RCS}} + Q_{\text{loss}} \tag{3}$$

$$|V^{\min}| \le |V_n| \le |V^{\max}| \quad n = 1,2,\ldots N_{\text{bus}} \tag{4}$$

$$P_{\text{dg}}^{\min} \le P_{\text{dg}} \le P_{\text{dg}}^{\max} \tag{5}$$

$$P_{\text{dg}} \le P_{\text{dg}}^{T,\max} < \min(P_{n,\text{D}}) \tag{6}$$

Here P_{sub} and Q_{sub} are real power and reactive powers of substations, respectively. P_{D} and Q_{D} are real and reactive power demands in distribution system. P_{loss} and Q_{loss} are real power loss and reactive power loss. Here RCS has real power loads (P_{RCS}) and reactive power load (Q_{RCS}). $V^{\min}$, $V^{\max}$, $P_{\text{dg}}^{\min}$, and $P_{\text{dg}}^{\max}$ are the lower voltage limit, upper voltage limit, DGs lower real power limit and DGs upper real power limit, respectively. $P_{\text{dg}}^{T,\max}$ is the maximum limit of total active power supplied by all DGs. $P_{n,\text{D}}$ real power demand at n^{th} node of distribution system.

2.1.2 | Stage II: Optimal sizing of RCS

After identifying the optimal locations of RCS, optimal locations and sizes of DGs, number of assigned EVs at each RCS calculated in Stage I are considered as input information to Stage 2. Based on this, arrival rate is calculated and is used in M1/M2/C queuing model for finding the waiting time in queue at RCS. In Stage II, optimal sizing of RCS has been done by determining the optimal number of connectors at each RCS locations. Installation cost of RCS (ICRCS) and waiting time (W_T) in queue at RCS were depends on the number of connectors at RCS. In Stage II, optimal number of connectors were determined by minimizing the ICRCS and W_T. Equation (7) shows objective function in Stage II, where feasible number of connectors (C) at each RCS were decision variables.

$$f(C) = \min(W_T, \text{ICRCS}) \tag{7}$$

Equation (8) is supporting the fact that every RCS should have minimum one connector, it is used in Stage II while determining the optimal number of connectors at RCS. Where, $CS_i^{\text{connector}}$ is the number of connectors at i^{th} RCS.

$$CS_i^{\text{connector}} \ge 1 \quad i = 1,2,..z(\text{number of RCS}) \tag{8}$$

2.2 | DG modelling

Modelling of DGs is necessary for the load flow studies. DGs can be modelled either as PQ mode or PV mode. In this article, DG is modelled in PQ mode that is, negative load model. Here, the DG reactive power output is calculated from Equation (9) with known quantities of real power output (P_{dg}) and power factor (pf).

$$Q_{\text{dg}} = P_{\text{dg}} \times \tan\left(\cos^{-1}(\text{pf})\right) \tag{9}$$

2.3 | RCS modelling

In this work, RCS is modelled in PQ mode. Real power load (P_i^{RCS}) and reactive power load (Q_i^{RCS}) due to EVs at i^{th} RCS are obtained by Equations (10) and (11), respectively. P_i^{RCS} depends on the total number of EVs (N_i^{EV}) at i^{th} RCS and rating of EV battery ($P_{\text{EV}}^{\max}$). The effective real and reactive power loads ($P_n^{\text{Effload}}, Q_n^{\text{Effload}}$) at n^{th} bus in distribution system are calculated using Equation (14) and (15), respectively. It is considered that CS is operating at 0.95 lag power factor.[11] Equations (12) and (13) are used to determine the connectors and capacity of i^{th} RCS, respectively. Here, R_{c} is the connector capacity, P_{evc} is the charging probability of EVs.

$$P_i^{\text{RCS}} = N_i^{\text{EV}} \times P_{\text{EV}}^{\max} \tag{10}$$

$$Q_i^{\text{RCS}} = P_i^{\text{RCS}} \times \tan\left(\cos^{-1}(\text{pf})\right) \tag{11}$$

$$\text{RCS}_i^{\text{connectors}} = \max(P_{\text{evc}}) \times N_i^{\text{EV}} \tag{12}$$

$$\text{RCS}_i^{\text{capacity}} = \text{RCS}_i^{\text{connectors}} \times R_{\text{c}} \tag{13}$$

$$P_n^{\text{Effload}} = P_n^{\text{load}} - P_n^{\text{dg}} + P_n^{\text{RCS}} \tag{14}$$

$$Q_n^{\text{Effload}} = Q_n^{\text{load}} - Q_n^{\text{dg}} + Q_n^{\text{RCS}} \tag{15}$$

2.4 | Network power loss

RCS integration results in high active power loss as there will be an increase in current flow through the branches. Furthermore, RCS location has a significant impact on distribution system performance. Power loss can be calculated from the feed forward and backward sweep load flow algorithm. Equation (16) gives the total network power loss at t^{th} hour. Daily power loss was calculated using Equation (17).

$$\text{ploss}(t) = \sum_{b=1}^{\text{nb}} (i_b)^2 \times (R_b) \tag{16}$$

$$P\text{loss} = \sum_{t=1}^{24} \text{ploss}(t) \tag{17}$$

where i_b is b^{th} branch current, R_b is b^{th} branch resistance, and nb is the total number of branches. Rapid charging stations (RCS) impose additional load on the network, resulting in increased power loss, and voltage magnitude degradation at the buses.

2.5 | Voltage deviation

Voltage variations beyond the permissible limits are produced by RCS loading. As a result, the system may become unstable. The voltage stability of the system is achieved by reducing the MVD and increasing the VSI. The load flow algorithm gives the voltage magnitude at each bus, Equation (18) gives the maximum value of voltage deviation ($\text{VD}_{\max}(t)$) at time t. MVD over a day can be calculated by Equation (19).

$$\text{VD}_{\max}(t) = \max(1 - v(i), t) \quad i = 1,2,3...N_{\text{distnodes}} \tag{18}$$

$$\text{MVD} = \sum_{t=1}^{24} \text{VD}_{\max}(t) \tag{19}$$

2.6 | Voltage Stability Index

VSI (Equation [20]) is one of the important factors that gives information about system voltage stability. Utility expects VSI at each bus to be near unity. VSI varies with loading that is, as the loading increases, VSI would reduce. The bus having maximum VSI (≤ 1) is strong, and is capable of taking extra load.

$$\text{VSI}_r = 2V_s^2V_r^2 - V_r^4 - 2V_r^2(P_rR(k) + Q_rX(k)) - |z|^2(P_r^2 + Q_r^2) \tag{20}$$

where VSI_r is VSI at receiving end of a line k, V_r and V_s are receiving end and sending end voltages, P_r and Q_r are real and reactive power at receiving end of line k, $R(k)$ and $X(k)$ are resistance and reactance of line k.

2.7 | EV user cost

When moving from an EV location to RCS, energy is lost. The EV user selects the closest CS available for charging. The best locations for RCS must take EV user behaviour into account when choosing the RCS to use. Minimization of the user cost of EVs is considered in the objective function while locating RCS.

Consider m ($m \in S$) RCSs dispersed at various sites ($C_1, C_2, ..C_s$). The transportation network is segmented into Z zones, with EVs assumed to be present at each zone's geometrical center. RCS can be placed at interconnected points of distribution network and transportation network in a coupled network. Figure 2 shows the considered test system, where each zone and feasible CS locations were identified by its coordinates that is, (x_{Z_1}, y_{Z_1}) and (x_{C_1}, y_{C_1}), respectively. In a test system, distribution network nodes are the possible locations for RCS placement. So, there is a need to find the distance between all zones to selected m CS locations in optimal planning. Equation (21) can determine the distance between the selected m CSs and each zone. Information about the distances between all zones and particular CSs is provided by D matrix Equation (22). Each element in DD matrix reflects the distance between the nearest RCS among the selected RCSs and the corresponding zones and is determined by the minimum value in each row of the D matrix using Equation (23). EVs located at the zones are assigned to nearest RCS.

$$d_{Z_1-C_1} = \sqrt{(x_{Z_1} - x_{C_1})^2 + (y_{Z_1} - y_{C_1})^2} \tag{21}$$

$$\text{D} = \begin{bmatrix} d_{Z_1-C_1} & d_{Z_1-C_2} & .. & d_{Z_1-C_m} \\ d_{Z_2-C_1} & d_{Z_2-C_2} & .. & d_{Z_2-C_m} \\ . & . & . & . \\ . & . & . & . \\ d_{Z_z-C_1} & d_{Z_z-C_2} & .. & d_{Z_z-C_m} \end{bmatrix} \tag{22}$$

$$\text{DD} = \begin{bmatrix} \min(d_{Z_1-C_1} d_{Z_1-C_2} .. d_{Z_1-C_m}) \\ \min(d_{Z_2-C_1} d_{Z_2-C_2} .. d_{Z_2-C_m}) \\ \min(....) \\ \min(....) \\ \min(d_{Z_z-C_1} d_{Z_z-C_2} .. d_{Z_z-C_m}) \end{bmatrix} \tag{23}$$

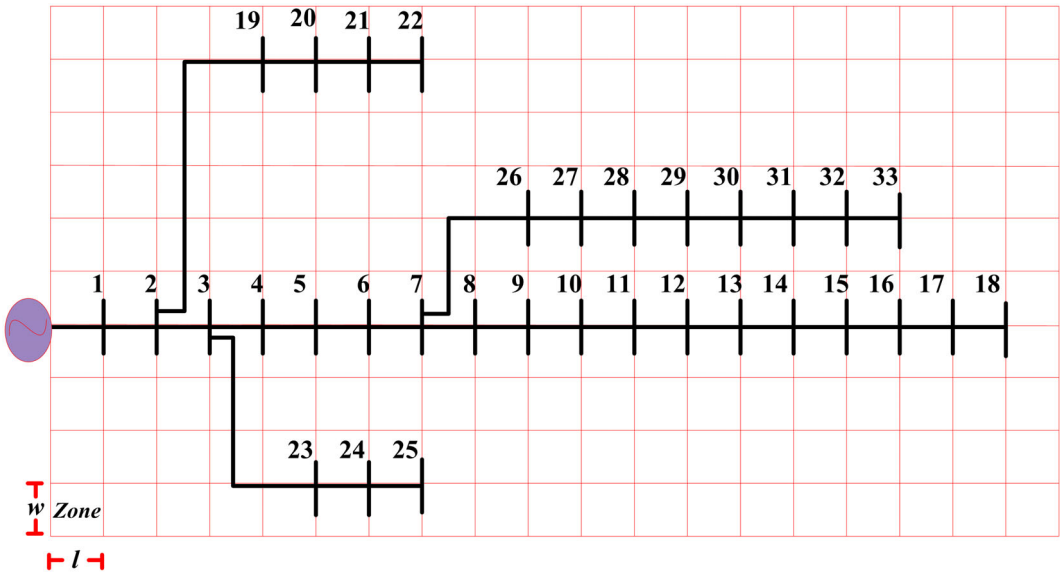

FIGURE 2 Test system (coupled network of transportation network with IEEE 33 bus radial distribution network).

$$\mathrm{EV}_{\mathrm{usercost}} = \sum_{n=1}^{z} \mathrm{DD}(i) \times N_i^{\mathrm{EV}} \times E_c \times P_e \tag{24}$$

Equation (24) gives the EV user cost. Here N_i^{EV} is the number of EVs getting charged from i^{th} RCS, E_c is the average energy consumption of EVs and P_e is the cost of electricity.

2.8 | Installation cost of RCS (ICRCS)

The installation cost of an RCS is important from a CS owner perspective. ICRCS depends on the number of connectors ($\mathrm{RCS}_i^{\mathrm{connectors}}$) at RCS, and is computed using Equation (25).

$$\begin{aligned}\mathrm{ICRCS}(i) = {} & C_{\mathrm{init}} + 25 \times C_{\mathrm{land}} \times \mathrm{RCS}_i^{\mathrm{connectors}} \\ & + C_{\mathrm{con}}\left(\mathrm{RCS}_i^{\mathrm{connectors}} - 1\right) \times Pc\end{aligned} \tag{25}$$

where C_{init} is initial investment cost, C_{land} is land cost, $\mathrm{RCS}_i^{\mathrm{connectors}}$ is number of connectors at i^{th} RCS, C_{con} is connector cost, and P_c is connector rating.

2.9 | RCS connector operation model

The M1/M2/C queuing model is taken into account in this study to describe the serviceability of CSs.[21] M1 denotes the rate of EV arrivals per hour, M2 is the rate of RCS connector service per hour, and C denotes the number of service points at the CS. EVs often drive up to a CS to charge their batteries. They arrive at a rate of λ/hour on average. It is modelled as a non-homogeneous Poisson process as it is time-dependent. Connectors are available in the RCS to charge the EV. These connectors perform the role of servers and charge the EVs at a service rate of μ/hour. In this case, the waiting line for EVs is assumed to be infinitely long. To ensure service to all EVs in the RCS, the arrival rate must always be lower than the service rate (Equation [27]).

$$\lambda(t) = N_{\mathrm{ev}}^{\mathrm{iCS}} \times P_{\mathrm{evc}} \tag{26}$$

$$\rho = \frac{\lambda(t)}{C\mu_t} < 1 \tag{27}$$

The probability of number of EVs charging at each RCS simultaneously is modelled using Equation (28).

$$p_t(n) = \frac{(C\rho)^n}{n!} \times p_t(0) \quad n = 1,2,3,\ldots,C \tag{28}$$

$$p_t(0) = \left[\sum_{s=0}^{C-1} \frac{(C\rho)^s}{s!} + \frac{(C\rho)^C}{C!}\frac{1}{(1-\rho)}\right]^{-1} \tag{29}$$

where $p_t(0)$ as expressed in above equations is the probability of no EV getting charged.

According to Little's equations, Equation (30) gives the expected number of EV users waiting at the RCS at t^{th} hour.

$$E_t[n] = p_t(0)\left[\frac{1}{(C-1)!}\left(\frac{\lambda_t}{\mu_t}\right)^C \frac{\lambda_t \mu_t}{(C\mu_t - \lambda_t)^2}\right] \quad (30)$$

Waiting time in queue of EV at t^{th} hour can be calculated using Equation (31). Total waiting time in a 24 hours period at all RCS is calculated using Equation (32)

$$W(t) = \frac{E_t[n]}{\lambda(t)} \quad (31)$$

$$W_T = \sum_{i=1}^{m}\sum_{t=1}^{24} W(t) \quad (32)$$

It is necessary to calculate the minimum and maximum limit for connectors at each RCS to satisfy Equation (27). The arrival rate at RCS is calculated using Equation (26). Equation (12) can be used to calculate the maximum number of connectors ($C^{\max}$) at RCS, while Equation (33) can be used to get the minimum number of connectors ($C^{\min}$).

$$\frac{\lambda^{\max}}{\mu} < C^{\min} \quad \lambda^{\max} \in \lambda(t) \quad (33)$$

3 | MULTI-OBJECTIVE OPTIMIZATION ALGORITHMS

Multi-objective optimization is preferable to identify the best solution for achieving multiple goals. Multiple-objective issues can be resolved using scalarization techniques and Pareto-based approaches. The weighted sum strategy is used in scalarization approaches to combine all the objectives into a single objective function. Here, a single objective is the sum of individual objectives, multiplied by weights according to their priority. However, this approach is not optimal for multi-objective problems with conflicting objectives. In this case, Pareto dominance-based multi-objective approaches provide the most efficient solutions.

3.1 | Non dominated sorting genetic algorithm

A multi objective optimization problem with conflicting objectives can be solved using NSGA II, proposed by Kalyan Deb in Reference 25. To achieve optimal Pareto front, crowding distance and dominance principle are used. Since the objectives are inherently conflicting, the best compromise solution is selected using a fuzzy min-max decision-making method.

3.2 | Multi objective Rao Algorithm (MORA)

Dominance principle and crowding distance analysis must be used to determine Pareto optimal solutions in a system with multiple objectives that are in conflict with each other. In this study, MORA proposed by Rao in 2021[26] was used to find the best solution. Fewer algorithmic parameters (population size and maximum iterations) make MORA simpler to understand and use.

The population of a feasible decision variable (P_o) with size (N) is initially generated at random. The rank and crowding distance were used to determine the best and worst solutions after evaluating the fitness function. New solutions (P_n) were determined using Equation (34). A set of solutions of size (N) was chosen from a set ($P_o UP_n$) based on rank and crowding distance after the evaluation of the fitness function for the new solution.

$$\begin{aligned} X'_{i,j,k} &= X_{i,j,k} + r1_{j,k}\left(X_{j,\text{best},k} - |\left(X_{j,\text{worst},k}\right)\right) \\ &+ r2_{j,k}\left(\left(|\, X_{i,j,k} \text{or} X_{r,j,k}\,|\right) - \left(X_{r,j,k} \text{or} X_{i,j,k}\right)\right) \end{aligned} \quad (34)$$

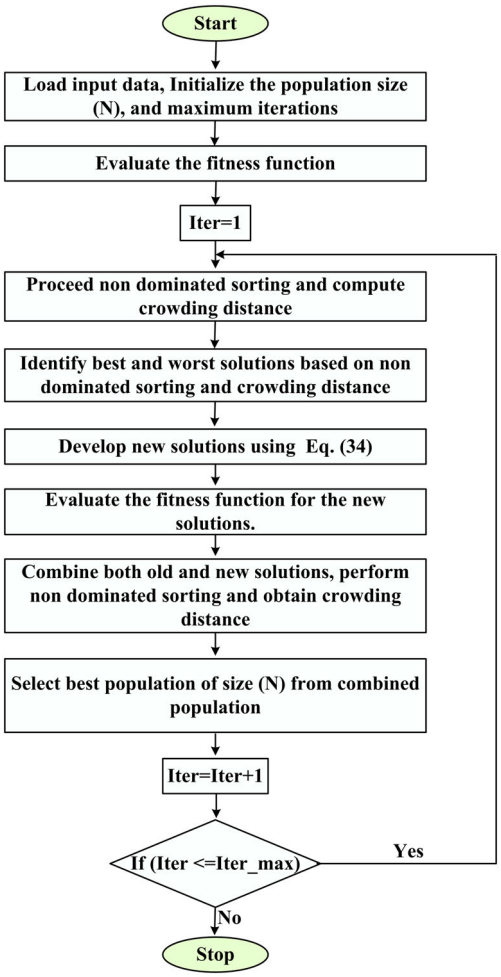

FIGURE 3 Flowchart of MORA[26] for the proposed problem.

Here $X'_{i,j,k}$ is the new solution of i^{th} candidate, j^{th} variable in k^{th} iteration. $X_{i,j,k}$ is the old solution of i^{th} candidate, j^{th} variable in k^{th} iteration, $r1, r2$ are random values between [0,1]. $X_{j,best,k}$ is the best value of j^{th} variable of X in k^{th} iteration. $X_{j,worst,k}$ is the worst value of j^{th} variable of X in k^{th} iteration. $X_{r,j,k}$ randomly selected r^{th} candidate, j^{th} variable in k^{th} iteration. The flowchart of MORA for optimal planning is shown in Figure 3 (Tables 1–3).

TABLE 1 Parameters of EV.

Parameters	Values
EV battery capacity	27.69 kWh
No of EVs	600
Avg. power consumption	0.142 kWh/km
Connector rating (P_c)	96 kW

TABLE 2 Cost coefficients of land.

Coefficients	Costs
C_{init}	70 000 $
C_{land}	240 $/m^2
C_{con}	280.33 $/kW

TABLE 3 Classification of connected loads in IEEE 33 bus RDS.

Residential loads	Commercial loads	Industrial loads
2, 3, 5, 6, 7, 8	4, 11, 12, 18	22, 26, 27, 28
9, 10, 13, 14, 15	19	29, 30, 31, 32
16, 17, 20, 23, 24	–	33

4 | SIMULATION RESULTS AND DISCUSSION

The effectiveness of the proposed method for RCS and DG optimal planning in coupled networks was evaluated by the proposed test system. The proposed test system is a coupled network of IEEE 33 bus distribution system superimposed on a 20×38 km^2 transportation area. The transportation area in chosen test system is divided into 190 zones with each zone having an area of 2 km^2. It is considered that EVs are located at the geometrical center of each zone, and the distribution of 600 EVs throughout 190 zones in the transportation area is represented in Table 4. In the first Stage, the best location for RCS and the best location and size for DGs were determined simultaneously. Queuing theory was employed in the second Stage to size RCS properly. In both stages, MORA was used to solve optimization problems with a population size of 30 and 100 iterations. The optimal results obtained by MORA were compared with the results obtained by NSGA-II algorithm. The parameters considered for NSGA-II in optimization are 30 population size, 100 maximum generations, crossover probability of 0.8, and mutation probability of 0.33.

Figure 4 shows the probability of EVs charging at RCS. Observations show that EVs do not charge before 5:00 AM and after 9:00 PM. The line and load data for IEEE 33 bus system were taken from Reference 5. There are 33 buses and 32 lines in the test system. Of the 33 buses, 17 carry residential loads, 9 carry industrial loads, and 5 carry commercial loads (Table 3). In this study, the variation in load was also taken into account, Figure 5 depicts the load demand variation over 24 hours. Simulations were carried out in the MATLAB 2014b software with the PC specification of Intel core i3 processor and 4 GB RAM.

TABLE 4 Assumed number of electric vehicles assigned to each of the 190 zones of transportation system.

1	4	3	1	5	1	1	2	3	4	4	5	5	4	2	5	3	3	4
3	4	2	4	1	3	3	1	5	5	4	4	2	1	2	4	5	1	4
3	5	4	1	1	5	4	5	4	4	3	1	3	3	5	2	5	5	2
4	1	2	2	5	2	2	4	4	4	5	4	2	3	5	2	2	5	1
4	3	4	4	4	5	4	1	4	3	4	4	4	1	2	1	5	3	4
2	4	5	3	3	4	2	3	3	5	3	4	3	3	1	5	4	2	1
5	5	4	2	2	2	4	4	5	5	2	5	4	2	2	3	3	3	2
5	5	4	2	4	4	3	5	5	4	1	1	1	5	3	4	3	3	3
1	4	3	1	1	1	4	2	1	3	5	4	4	2	2	1	4	3	3
4	1	1	1	5	1	4	3	5	2	1	2	4	3	5	4	1	5	4

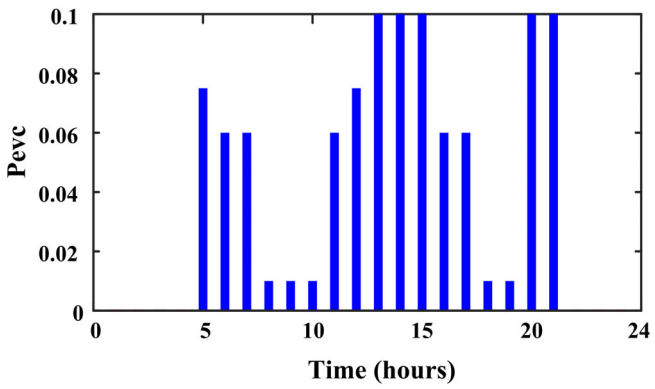

FIGURE 4 Electric vehicle charging probability.

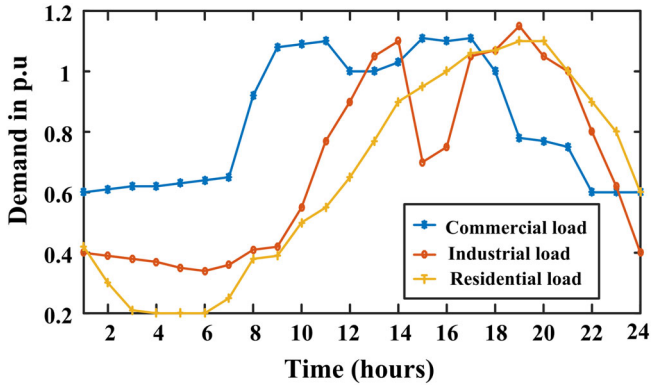

FIGURE 5 Plot of load demands of various types of loads.

4.1 | Base case

The analysis of test system was done without integrating RCS and DGs in base case. The feed forward-backward sweep algorithm was employed to analyse the network, because the test system consists of IEEE 33 bus radial distribution system, which has high R/X ratio. It reported a base case active power loss of 2811 kW, MVD of 1.5816 (p.u.), and voltage stability index (VSI_{min}) of 0.6479. Figure 6 shows a plot of voltage profiles of IEEE 33 bus RDS for 24 hours at each bus. It is observed from Figure 6 that at 17th hour the system's minimum voltage is 0.8968 (p.u.) at the 18th bus of IEEE 33 Bus RDS.

4.2 | Stage 1: Optimal location of RCS and optimal location and sizing of DGs

MORA was used to find the optimal locations for RCS and optimal locations and sizes for DGs in the first stage. Two scenarios, with three cases in each, were used to analyse the optimal planning.

4.2.1 | Scenario 1: Optimal planning of RCS in coupled network

In this scenario, the analysis of network was done by integrating RCS. In Scenario 1, three cases were

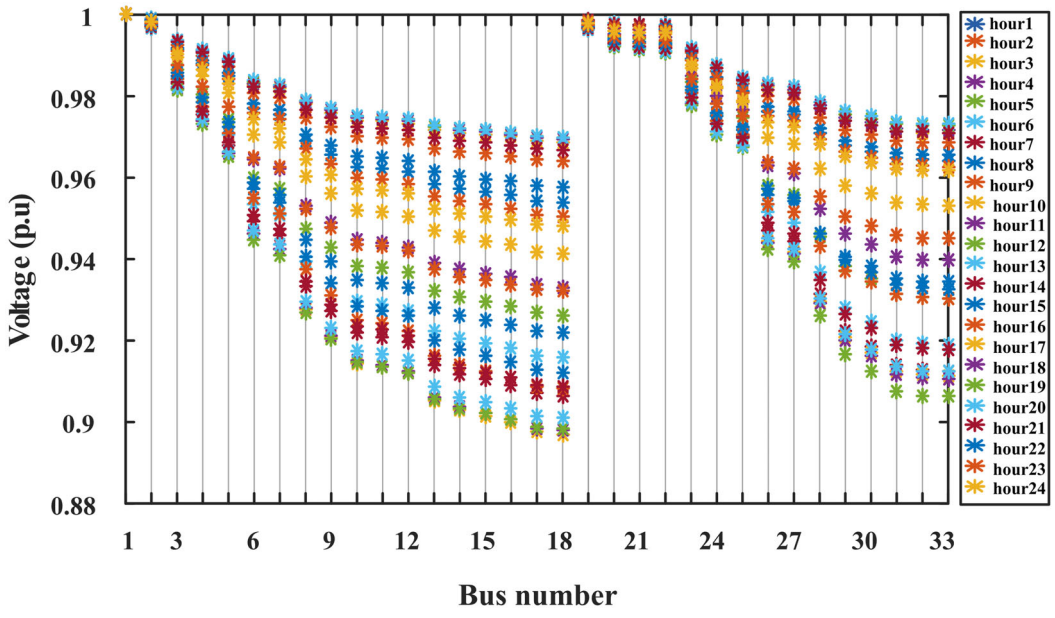

FIGURE 6 Plot of voltage profiles at each bus of IEEE 33 bus RDS for 24 hours without the integration of RCS and DGs.

considered to analyse the network for optimal planning of RCS. MORA algorithm was applied in each case to get the optimal fronts.

Case 1. Optimal planning of RCS by minimizing Ploss, MVD, and EVUC.

Case 2. Optimal planning of RCS by minimizing Ploss, $1/\text{VSI}_{\text{min}}$, and EVUC.

Case 3. Optimal planning of RCS by minimizing Ploss, MVD, $1/\text{VSI}_{\text{min}}$, and EVUC.

Fuzzy min max decision making technique was employed to achieve the compromised optimal solution. The optimal Pareto front in Case 3 by MORA is shown in Figure 7. Optimal locations of RCS and the corresponding objective function parameters are given in Tables 5 and 6, respectively.

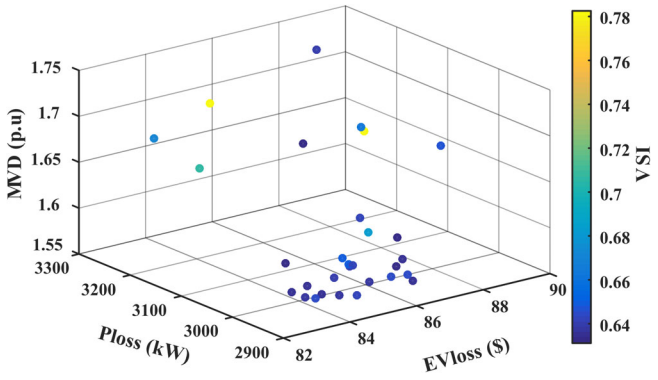

FIGURE 7 Optimal Pareto-front of Ploss, MVD, VSI, and EVUC by MORA in Case 3.

From Table 6, it is observed that MORA algorithm yielded better objective parameters compared to NSGA II with Ploss of 3560.3 kW, MVD of 1.7217 (p.u), VSI_{min} of 0.6182, and EVUC of 60.0221 $ in Case 1. The maximization of VSI in place of MVD resulted in improvement of voltage profile in Case 2. Better values of Ploss, MVD, and VSI_{min} were obtained by MORA in Case 2. However, highest EVUC was encountered by MORA (EVUC 88.6718 $) compared to NSGA II (EVUC 60.9249 $). The consideration of VSI maximization along with minimization of Ploss, MVD, and EVUC resulted in better voltage profile (MVD, VSI) and Ploss in Case 3 compared to all cases in Scenario 1. In Case 3, MORA yielded Ploss of 2997.1 kW, MVD of 1.5898 (p.u), VSI_{min} of 0.6464, and EVUC 86.7004 $. From Figures 8 and 9, it is observed that, the presence of RCS in the test system resulted in reduction of system minimum voltage to 0.8963 (p.u) and 0.8951 (p.u) at 18^{th} bus in 17^{th} hour by MORA and NSGA II algorithms, respectively compared to base case (0.8968 (p.u)). From Scenario 1, it is clear that though the RCS are placed at proper locations in the distribution network, it resulted in increased power loss that is, 1.07% of Base case (Ploss) and deteriorated voltage profile.

4.2.2 | Scenario 2: Concurrent optimal planning of RCS and DGs

Though the RCSs are located at optimal places, loading due to RCS would reduce the performance of the distribution system. To solve the above issue, Renewable type DGs of size 5 kW to 1 MW placement in distribution

TABLE 5 Optimal locations of RCS and the number of EVs assigned to RCS in Scenario 1 by NSGA II and MORA for different cases.

	NSGA II[25]		MORA	
Case no.	**RCS location**	**Number of EVs**	**RCS location**	**Number of EVs**
Case 1	2, 23, 27	150, 69, 381	2, 19, 27	134, 70, 396
Case 2	2, 22, 27	165, 77, 358	2, 19, 24	103, 198, 299
Case 3	2, 19, 23	102, 235, 263	2, 19, 22	171, 57, 372

TABLE 6 Objective function parameters in Scenario 1 by NSGA II and MORA for different cases.

	NSGA II[25]				MORA			
Case no.	**Ploss (kW)**	**MVD (p.u)**	VSI_{min}	**EVUC ($)**	**Ploss (kW)**	**MVD (p.u)**	VSI_{min}	**EVUC ($)**
Case 1	3572.8	1.7223	0.6182	60.7222	3560.3	1.7217	0.6182	60.0221
Case 2	3499.8	1.7093	0.6219	60.9249	3124.5	1.6124	0.6424	88.6718
Case 3	3026	1.6093	0.6430	94.2015	2977.1	1.5898	0.6464	86.7004

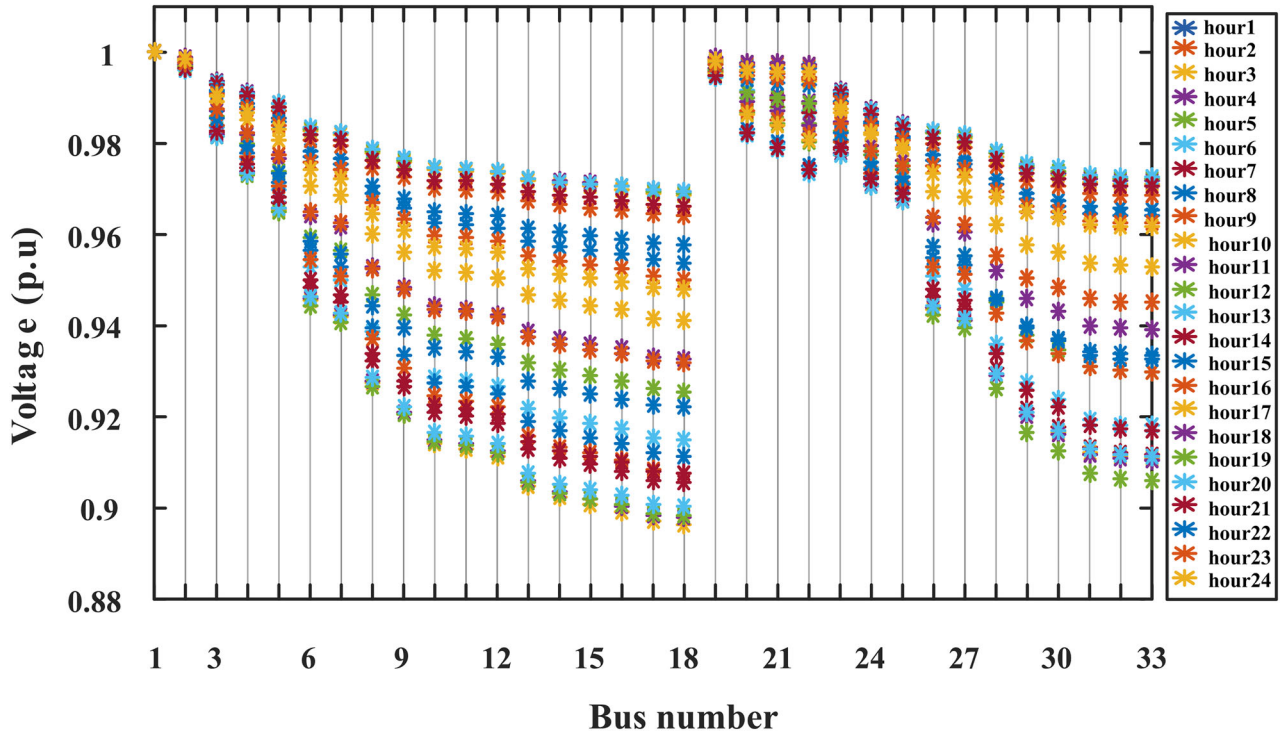

FIGURE 8 Plot of voltage profiles at each bus of IEEE 33 bus RDS for 24 hours with the integration of RCS by MORA in Case 3.

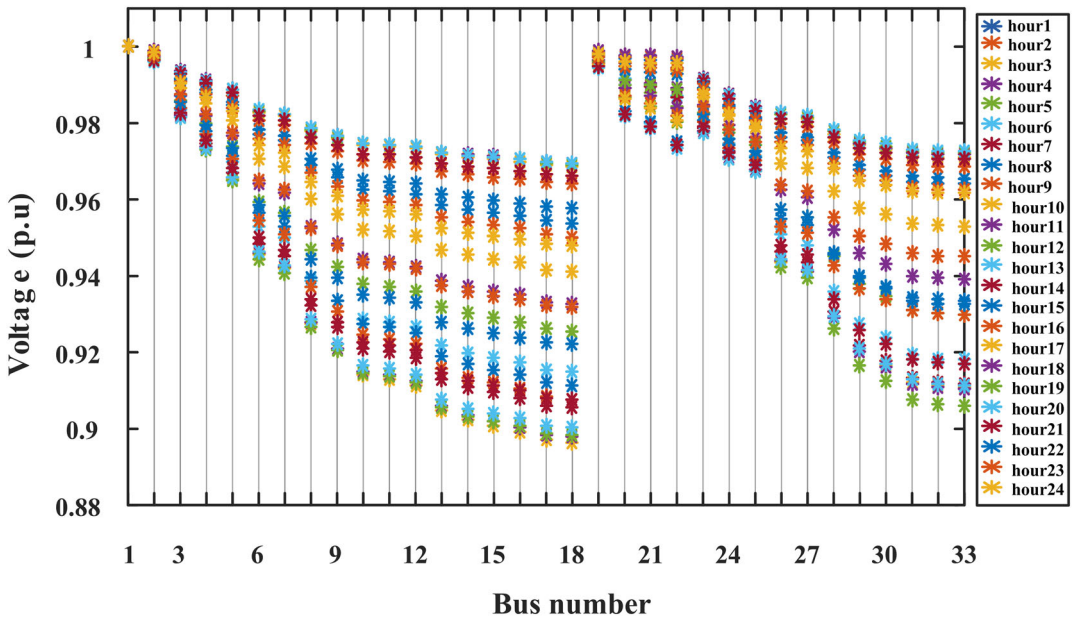

FIGURE 9 Plot of voltage profiles at each bus of IEEE 33 bus RDS for 24 hours with the integration of RCS by NSGA II in Case 3.

system was adopted in this article in Scenario 2. The distribution system has a minimum active power demand of 1420 kW at 4^{th} hour (Figure 10). To prevent reverse power flow, the total active power supplied by DGs is limited to less than or equal to 1400 kW. Three cases were considered in this scenario to analyse the network.

Case 4. Concurrent optimal planning of RCS and DGs in coupled network by minimizing the Ploss, EVUC, and MVD.

Case 5. Concurrent optimal planning of RCS

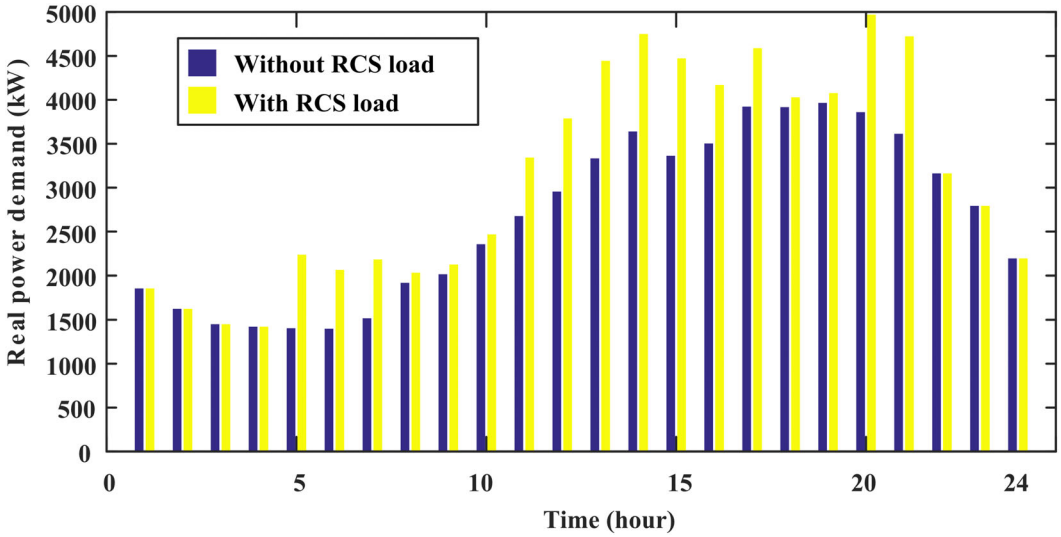

FIGURE 10 Daily real power demand with and without RCS load.

and DGs in coupled network by minimizing the Ploss, EVUC, and $1/VSI_{min}$.

Case 6. Concurrent optimal planning of RCS and DGs in coupled network by minimizing the Ploss, EVUC, $1/VSI_{min}$, and MVD.

MORA and NSGA-II algorithms were applied on the test system to obtain optimal locations and sizes of RCS and DGs. Fuzzy min max decision making was employed to obtain best compromised solution from optimal fronts. The optimal front by MORA is shown in Figure 11. The optimal locations of RCS and assigned EVs at RCS obtained by MORA and NSGA II algorithms are mentioned in Table 7. Optimal locations and sizes of DGs obtained by MORA and NSGA II are given in Table 8. Objective parameters obtained in various cases by MORA and NSGA II algorithms in Scenario 2 are listed in Table 9.

Table 9 shows that the integration of DG reduced power loss, MVD, and improved VSI of distribution system compared to Scenario 1. In Case 4, MORA algorithm led to lower power loss (1228.1 kW), MVD (0.6955 [p.u]), and EVUC (52.5431 $) compared to NSGA II. However, better VSI_{min} (0.7870) was obtained by NSGA II.

In Case 5, lower Ploss (1274.2 kW), MVD (0.7035 [p.u]), and better VSI_{min} (0.7797) were obtained by MORA compared to NSGA II. Furthermore, the maximization of VSI along with the minimization of Ploss and EVUC resulted in better values of VSI_{min} (0.7797) in Case 5 compared to Case 4 (VSI_{min} [0.7785]) by MORA. Collective consideration of Ploss, MVD, VSI_{min} and EVUC parameters in objective function resulted in lowest

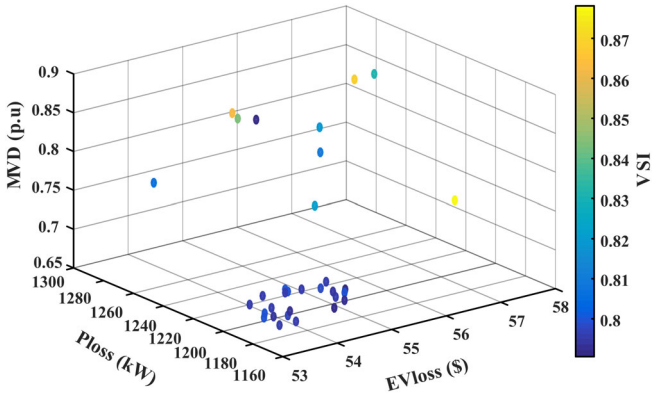

FIGURE 11 Optimal Pareto-front of Ploss, MVD, VSI, and EVUC by MORA in Case 6.

Ploss (1182.3 kW), MVD (0.6864 [p.u]), and better value of VSI_{min} of 0.7946 and EVUC of 53.4033 $ in Case 6 by MORA. The system minimum voltage is 0.9432 (p.u) in Case 6, at bus 33 in 17th hour (Figure 12). It is more compared to 0.9428 (p.u) by NSGA-II in Case 6 (Figure 13). The voltage at 18th bus 17th hour improved to 0.9461 (p.u) compared to base case (0.8968 [p.u]).

The objective function parameters of best cases from Scenario 1 (Case 3), Scenario 2 (Case 6) and base case are listed in Table 10. Table 10 shows concurrent optimal planning of RCS and DGs (Case 6) solved the issues caused by the integration of RCS (Case 3). Ploss was 42% of base case Ploss in Case 6 where as 107% in Case 3. MVD was 43.17% of base case MVD in Case 6 where as 100.6% in Case 3.

Maximum value of VSI_{min} was obtained in Case 6 compared to base case and Case 3. Furthermore, lowest

TABLE 7 Optimal locations of RCS and the number of EVs assigned to RCS in Scenario 2 by NSGA II and MORA for different cases.

	NSGA II[25]		MORA	
Case no.	**RCS location**	**Number of EVs**	**RCS location**	**Number of EVs**
Case 4	2, 21, 32	178, 138, 284	2, 22, 32	196, 135, 269
Case 5	2, 21, 30	167, 107, 326	2, 21, 29	163, 33, 338
Case 6	2, 21, 33	183, 157, 260	2, 22, 33	201, 151, 248

TABLE 8 Optimal locations and sizes of DGs in Scenario 2 by NSGA II and MORA for different cases.

	NSGA II[25]		MORA	
Case no.	**DG location**	**DG size**	**DG location**	**DG size**
Case 4	18, 30, 33	383, 246, 748	9, 18, 33	280, 300, 804
Case 5	15, 18, 33	708, 226, 443	11, 17, 32	280, 250, 854
Case 6	17, 30, 32	383, 276, 718	14, 30, 32	483, 103, 804

TABLE 9 Objective function parameters in Scenario 2 by NSGA II and MORA for different cases.

	NSGA II[25]				MORA			
Case no.	**Ploss (kW)**	**MVD (p.u)**	**VSI_{min}**	**EVUC ($)**	**Ploss (kW)**	**MVD (p.u)**	**VSI_{min}**	**EVUC ($)**
Case 4	1272.4	0.7003	0.7870	53.2199	1228.1	0.6955	0.7785	52.5431
Case 5	1408.3	0.7267	0.7619	53.3290	1274.2	0.7035	0.7797	54.7130
Case 6	1218.2	0.6964	0.7933	54.4474	1182.3	0.6864	0.7946	53.4033

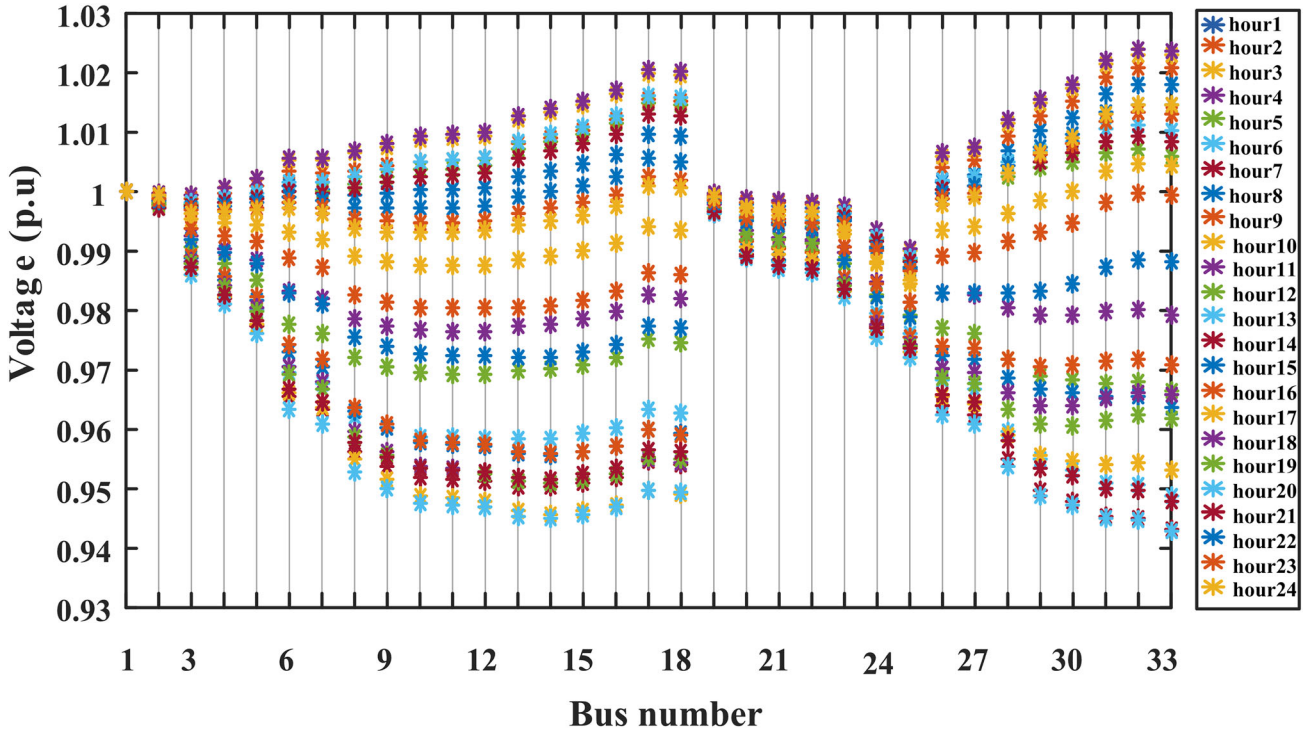

FIGURE 12 Plot of voltage profiles at each bus of IEEE 33 bus RDS for 24 hours with the integration of RCS and DGs by MORA in Case 6.

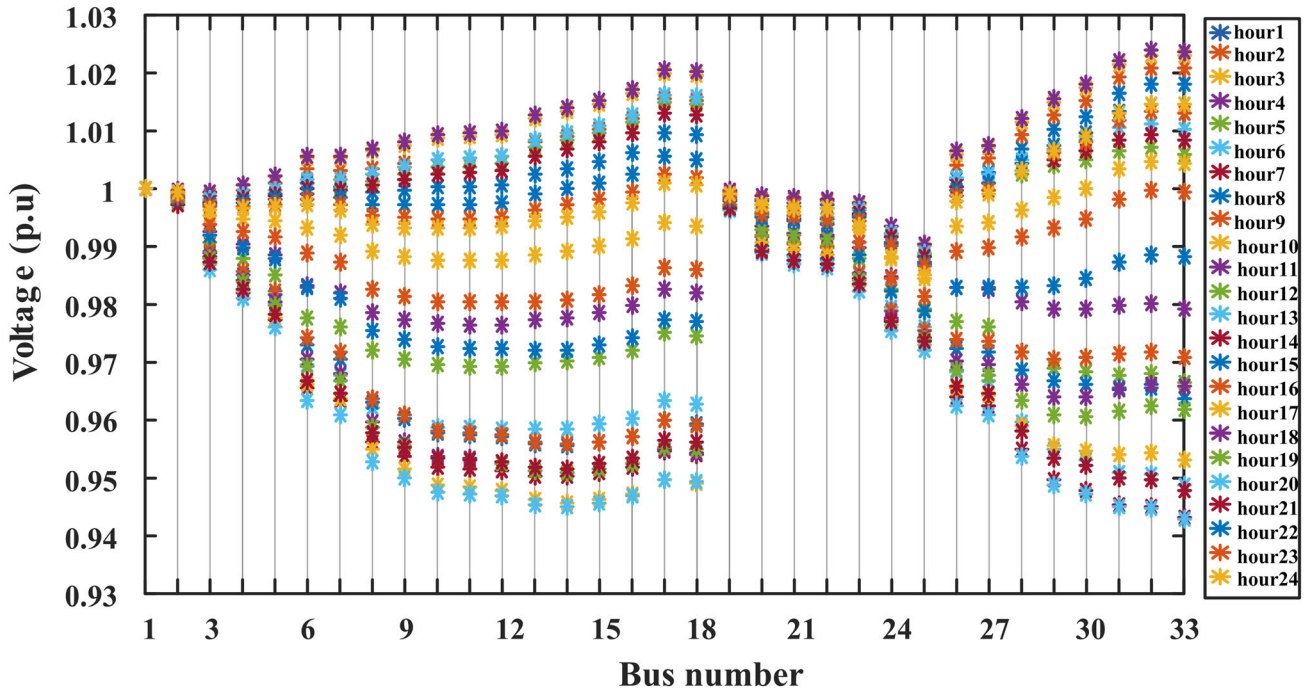

FIGURE 13 Plot of voltage profile at each bus of IEEE 33 bus RDS for 24 hours with the integration of RCS and DGs by NSGA II in Case 6.

TABLE 10 Comparison of objective function parameters in base case, Case 3, and Case 6.

Case no.	Ploss (kW)	MVD (p.u)	VSI_{min}	EVUC ($)
Base case	2811	1.5816	0.6479	–
Case 3	2977.1	1.5898	0.6464	86.7004
Case 6	1182.3	0.6864	0.7946	53.4033

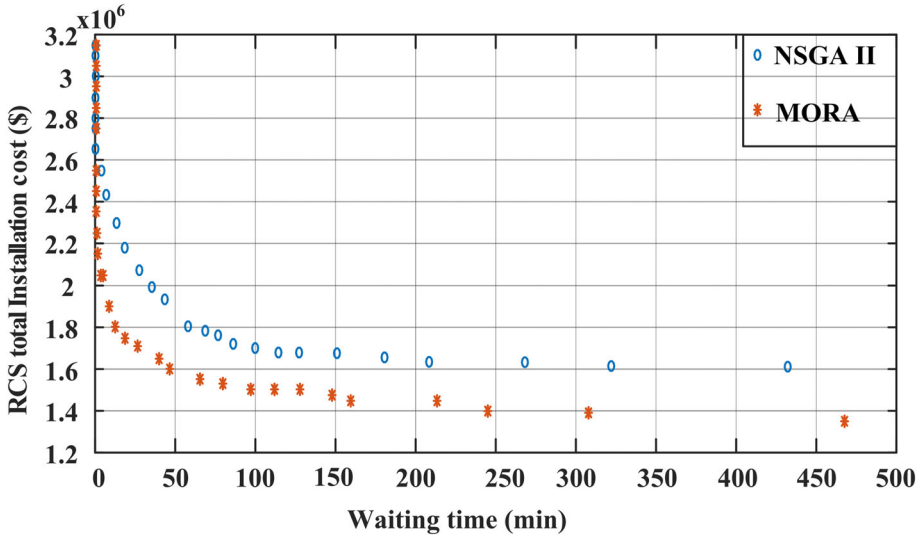

FIGURE 14 Plot of waiting time and RCS total installation cost by MORA and NSGA II.

TABLE 11 Comparison of results in traditional and proposed approach in Stage 2.

Parameter	Traditional approach	Proposed approach	
		NSGA II[25]	MORA
Optimal no of connectors	20, 15, 25	9, 13, 15	10, 8, 14
RCS capacity (kW)	1920, 1440, 2400	864, 1248, 1440	960, 768, 1344
ICRCS ($)	3.15×10^6	2.01×10^6	1.75×10^6
W_T (min)	0.0088	35.5202	27.9801

EVUC (53.4033 $) was obtained in Case 6 compared to Case 3. Therefore, the proposed method of integration of DGs along with the RCS is a viable method to optimally locate RCS without losing the distribution system performance. Furthermore, selecting optimal number of connectors at each RCS is necessary to minimize the installation cost of RCS and waiting time in queue at RCS. This would benefit the RCS owner economically. To achieve this goal, the optimal number of connectors were calculated in Stage 2.

4.3 | Stage 2: Optimal sizing of RCS

The number of connectors at RCS decides its size, cost, and waiting time for EVs to be charged at RCS. In the literature, Equations (12) and (13) were used to calculate the connectors at RCS and RCS capacity. However, Equation (12) gives maximum connectors at RCS. Consideration of maximum connectors at RCS results in high installation cost and less waiting time in queue. However, it is not feasible. Hence, it is necessary to determine optimal number of connectors.

From Stage 1, it is observed that in Case 6 better objective parameters are obtained by MORA. In Case 6, three RCS were optimally located at 2nd, 22nd, and 33rd buses of distributions system with each assigned EVs of 201, 151, and 248, respectively (Figure 14).

To employ queue theory, arrival rate ($\lambda(t)$) at each RCS and service rate of connector is required. Here, Arrival rate ($\lambda(t)$) at RCS is time dependent, and it is obtained by Equation (26). EV battery takes 22 minutes to get 85% charge.[21] Hence service rate μ/hour of 2.73/hour was considered in this article. Here the number of connectors (C) at each RCS is a variable, its minimum $\left(C^{\min}\right)$ and maximum $\left(C^{\max}\right)$ limits are calculated according to Equations (33) and (27), respectively. NSGA II and MORA algorithms were applied to obtain the compromised optimal feasible solution for sizing of RCS with C limits of $C^{\min} = [8,6,10]$ and $C^{\max} = [20,15,25]$. Fuzzy min max decision making was used to find the best solution among solutions from Pareto front.

Table 11 shows that, traditionally 20, 15, and 25 connectors were installed at RCS 1, RCS 2, and RCS 3, respectively. This resulted in maximum installation cost of $3.15 \times 10^6$$ and minimum waiting time in queue of 0.0088 minutes, that is, approximately no waiting time in queue. However, it is not economical for the owner of RCS because of which waiting time was considered in the proposed approach. NSGA II using the proposed approach yielded $2.01 \times 10^6$$ installation cost and 36.96 minutes of waiting time in queue for 9, 13, and 15 connectors at RCS 1, RCS 2, and RCS 3, respectively. Best compromised objective parameters of $1.75 \times 10^6$$ installation cost and 27.9801 minutes of waiting time in queue were obtained with 10, 8, and 14 connectors by MORA. These optimal connectors decided the size of RCS 1 as 960 kW, RCS 2 as 768 kW, and RCS 3 as 1344 kW by MORA. The plot between waiting time in queue and installation cost by NSGA II and MORA (Figure 13) shows the effectiveness of MORA in achieving optimal results.

5 | CONCLUSION

The planning of CS should be of use to electrical network, EV user, and CS owner. Though the RCS might be located at proper places, RCS integration would raise power loss and VD in distribution system. Consideration of EV user loss, RCS installation cost, and waiting time in queue at RCS plays a vital role in obtaining optimal locations for RCS, and these are in conflicting in nature. To address the above issues, this article proposed a two-stage approach to determine the optimal size and locations of RCS and DGs using Pareto based multi objective approach. Optimal location of RCS and optimal location and size of DGs are determined by minimizing power loss, voltage deviation, EV user cost, and maximizing the VSI in the first stage. M1/M2/C queuing model was used for finding the waiting in queue at RCS. Minimization of waiting time and installation cost of RCS were considered as objectives to determine the optimal number of connectors at RCS in

second stage. During the analysis, the variation of various types of loads and variation of probability of charging of EVs was considered. The optimization problem was solved by MORA and NSGA II. The advantages of metaphor-less, few parameters and ability to move candidate solution towards the best solution and away from the worst solution of MORA ensured faster convergence and better performance, and was verified by NSGA II algorithm. The integration of reactive power compensating devices along with RCS and DGS to improve the performance of the distribution system in coupled network would be potential areas for future research.

DATA AVAILABILITY STATEMENT

The data that support the findings of this study are available from the corresponding author upon reasonable request.

ORCID

Vutla Vijay https://orcid.org/0000-0002-1187-0170

REFERENCES

1. Ahmad F, Iqbal A, Ashraf I, Marzband M, Khan I. Optimal location of electric vehicle charging station and its impact on distribution network: a review. *Energy Rep*. 2022;8:2314-2333.
2. Khalid MR, Alam MS, Sarwar A, Asghar MSJ. A comprehensive review on electric vehicles charging infrastructures and their impacts on power-quality of the utility grid. *ETransportation*. 2019;1:100006.
3. Luo C, Huang Y-F, Gupta V. Placement of EV charging stations balancing benefits among multiple entities. *IEEE Trans Smart Grid*. 2015;8(2):759-768.
4. Boddapati V, Rakesh Kumar A, Prakash DB, Arul Daniel S. Design and feasibility analysis of a solar PV and biomass-based electric vehicle charging station for metropolitan cities (India). *Distrib Gener Altern Energy J*. 2022;37(3):793-818.
5. Deb S, Tammi K, Kalita K, Mahanta P. Impact of electric vehicle charging station load on distribution network. *Energies*. 2018;11(1):178.
6. Shariff SM, Alam MS, Hameed S, et al. A state of the art review on the impact of fast EV charging on the utility sector. *Energy Storage*. 2022;4(4):e300.
7. Babu, Ponnam Venkata K, Swarnasri K. Multi-objective optimal allocation of electric vehicle charging stations in radial distribution system using teaching learning based optimization. *Int J Renew Energy Res*. 2020;10(1):366-377.
8. Zeb MZ, Imran K, Khattak A, et al. Optimal placement of electric vehicle charging stations in the active distribution network. *IEEE Access*. 2020;8:68124-68134.
9. Ahmad F, Iqbal A, Ashraf I, Marzband M, Khan I. The optimal placement of electric vehicle fast charging stations in the electrical distribution system with randomly placed solar power distributed generations. *Distrib Gener Altern Energy J*. 2022;37:1277-1304.
10. Fokui WS, Tounsi MJS, Ngoo L. Optimal placement of electric vehicle charging stations in a distribution network with randomly distributed rooftop photovoltaic systems. *IEEE Access*. 2021;9:132397-132411.
11. Gampa SR, Jasthi K, Preetham Goli DD, Bansal RC. Grasshopper optimization algorithm based two stage fuzzy multiobjective approach for optimum sizing and placement of distributed generations, shunt capacitors and electric vehicle charging stations. *J Energy Storage*. 2020;27:101117.
12. Bilal M, Rizwan M, Alsaidan I, Almasoudi FM. AI-based approach for optimal placement of EVCS and DG with reliability analysis. *IEEE Access*. 2021;9:154204-154224.
13. Mukherjee V. Intelligent electric vehicles charging coupled demand response of isolated microgrid. *Energy Storage*. 2022;4(4):e326.
14. Kathiravan K, Rajnarayanan PN. Application of AOA algorithm for optimal placement of electric vehicle charging station to minimize line losses. *Electr Pow Syst Res*. 2023;214:108868.
15. Ferro G, Minciardi R, Parodi L, Robba M. Optimal planning of charging stations in coupled transportation and power networks based on user equilibrium conditions. *IEEE Trans Autom Sci Eng*. 2021;19(1):48-59.
16. Amer A, Azzouz MA, Azab A, Awad ASA. Stochastic planning for optimal allocation of fast charging stations and wind-based DGs. *IEEE Syst J*. 2020;15(3):4589-4599.
17. Sa'adati R, Jafari-Nokandi M, Saebi J. Allocation of RESs and PEV fast-charging station on coupled transportation and distribution networks. *Sustain Cities Soc*. 2021;65:102527.
18. Othman AM, Gabbar HA, Pino F, Repetto M. Optimal electrical fast charging stations by enhanced descent gradient and Voronoi diagram. *Comput Electr Eng*. 2020;83:106574.
19. Pal A, Bhattacharya A, Chakraborty AK. Allocation of electric vehicle charging station considering uncertainties. *Sustain Energy, Grids Netw*. 2021;25:100422.
20. Sadhukhan A, Ahmad MS, Sivasubramani S. Optimal allocation of EV charging stations in a radial distribution network using probabilistic load modeling. *IEEE Trans Intell Transp Syst*. 2021;23(8):11376-11385.
21. Hafez O, Bhattacharya K. Queuing analysis based PEV load modeling considering battery charging behavior and their impact on distribution system operation. *IEEE Trans Smart Grid*. 2016;9(1):261-273.
22. Uslu T, Kaya O. Location and capacity decisions for electric bus charging stations considering waiting times. *Transp Res D Transp Environ*. 2021;90:102645.
23. Asna M, Shareef H, Achikkulath P, Mokhlis H, Errouissi R, Wahyudie A. Analysis of an optimal planning model for electric vehicle fast-charging stations in Al Ain City, United Arab Emirates. *IEEE Access*. 2021;9:73678-73694.
24. Deb S, Tammi K, Gao X-Z, Kalita K, Mahanta P, Cross S. A robust two-stage planning model for the charging station placement problem considering road traffic uncertainty. *IEEE Trans Intell Transp Syst*. 2021;23:6571-6585.
25. Deb K, Pratap A, Agarwal S, Meyarivan TAMT. A fast and elitist multiobjective genetic algorithm: NSGA-II. *IEEE Trans Evol Comput*. 2002;6(2):182-197.
26. Rao RV, Keesari HS. Rao algorithms for multi-objective optimization of selected thermodynamic cycles. *Eng Comput*. 2021;37(4):3409-3437.

AUTHOR BIOGRAPHIES

Vutla Vijay received MTech from JNTU Kondagattu, Jagityal, Karimnagar in 2018. Currently, he is a research scholar in the Department of Electrical Engineering at NIT Warangal. His present research is in the area of optimal planning of DGs and electric vehicle charging station. His present research is in the area of AI applications to Power and Energy System.

Chintham Venkaiah received the PhD degree in Electrical Engineering from the National Institute of Technology (NIT) Warangal in 2014. Currently, he is Professor in the Department of Electrical Engineering at NIT Warangal. His present research is in the area of AI applications to Power and Energy System, Economics and Financing Renewable Energy Technologies.

D. M. Vinod Kumar obtained his BE (Electrical) and MTech (Power Systems) degrees from Osmania University, Hyderabad, during 1979 and 1981, respectively. He obtained his PhD degree from IIT Kanpur in the year 1996. During 2002–2003, he was Post Doctoral Fellow at Howard University, Washington DC, USA. His areas of interest are Power systems Operation and Control, Power System Stability and Security, AI techniques for Power System and Renewable Energy Systems. He was a Professor (HAG) of Electrical Engineering at NIT, Warangal.

How to cite this article: Vijay V, Venkaiah C, Kumar DMV. Multi objective queue theory based optimal planning of rapid charging stations and distributed generators in coupled transportation and distribution network. *Energy Storage*. 2024; 6(1):e484. doi:10.1002/est2.484